ARTICLES

Functionalized Pentacene Derivatives for Use as Red Emitters in Organic Light-Emitting Diodes

Mason A. Wolak, Bo-Bin Jang, Leonidas C. Palilis, and Zakya H. Kafafi*

U.S. Naval Research Laboratory, Code 5615, Washington, D.C. 20375

Received: July 28, 2003; In Final Form: February 12, 2004

A series of three pentacene derivatives featuring substituted aryl groups at the 6,13-position, namely, 6,13-diphenylpentacene, 6,13-bis(2,6-dimethylphenyl)pentacene, and 6,13-bis(4-*tert*-butylphenyl)pentacene, have been synthesized and characterized. The optical properties of each compound have been determined in solution and in the solid state. Films containing the pentacene derivatives dispersed in tris(quinolin-8-olato)aluminum-(III) (Alq_3) emit in the red with small contribution from the Alq_3 host, signaling efficient energy transfer from host to guest molecules. The absolute photoluminescence quantum yield (ϕ_{PL}) of composite films is ∼30−32% at optimum dopant concentration. Organic light-emitting diodes based on these composite films as the active emitting layers have been fabricated and characterized. External electroluminescence quantum efficiencies near the theoretical limit have been achieved.

Introduction

Displays utilizing organic light-emitting diodes (OLEDs) as active pixel elements are very promising and may soon replace the competing technology based on liquid crystals. They offer facile color tunability, bright self-emission, and wider viewing angles than liquid crystal displays (LCDs).[1,2] Although efficient blue and green OLEDs have already been developed,[3] efficient red OLEDs with good color purity (narrow emission) that are stable over a wide range of current densities remain elusive. The first practical red OLEDs were reported by Tang et al.[4] and contained DCM, a pyran-based fluorescent dye. Various new pyran dyes have since been developed and incorporated in devices, but they often feature broad emission that results in poor color chromaticity.[5−7] Recently, many red emitting phosphorescent compounds based on organoplatinum,[8] -ruthenium,[9] and -iridium[10−13] complexes have been incorporated in OLEDs. Phosphorescent dyes are attractive because they make use of the more highly populated triplet excited state for emission[14,15] and therefore yield impressive external electroluminescence (EL) quantum efficiencies at low current densities. Unfortunately, these high EL quantum efficiency values experience rapid decline at high current densities due to triplet−triplet annihilation and/or exciton-carrier quenching.[16] Electric field-assisted dissociation of singlet excitons have been reported at high voltage.[17] Some fluorescent guest molecules, such as DCJTB (4-dicyanomethylene)-2-*tert*-butyl-6-(1,1,7,7-tetramethyljulolidyl-9-enyl)-4*H*-pyran), undergo current-induced fluorescent quenching at relatively low current densities.[18]

Recently, a wide variety of new substituted pentacenes have been prepared in an effort to tailor properties such as crystal packing, solubility, charge transport, and the color and efficiency of luminescence.[19−23] These derivatives have been used in thin film transistors,[24] as photoresponsive conducting single crystals,[25] and in OLEDs.[26] Previously reported 6,13-diphenylpentacene[27,28] (DPP, **1**) is modestly fluorescent in chloroform

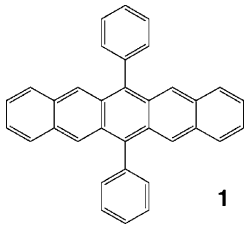

1

solution (λ_{em} = 610 nm) but exhibits no emission in neat thin films. Photoluminescence (PL) based primarily on DPP was attained by dispersing DPP in tris(quinolin-8-olato)aluminum-(III) (Alq_3), via efficient host to guest Förster energy transfer.[29] Composite films containing 0.55 mol % DPP displayed an absolute photoluminescence quantum yield (ϕ_{PL}) of 0.30. OLEDs based upon these composite films were fabricated and yielded external EL quantum efficiencies up to 1.3% that were (color) stable across a wide range of current densities.[26]

In this study, we investigate the effect of functionalizing the phenyl groups of DPP (**1**) in the ortho- and para-positions on its optical and electronic properties. We have synthesized two pentacene derivatives that feature *tert*-butyl substitution at the para-position or methyl substitution at both ortho-positions of the phenyl group relative to the point of attachment to the pentacene unit. In addition, we fabricated and characterized red-emitting OLEDs based on these fluorescent pentacene derivatives.

* To whom correspondence should be addressed. Phone: 2027679529. Fax: 2024048114. E-mail: kafafi@ccs.nrl.navy.mil.

10.1021/jp036199u CCC: $27.50
Published on Web 04/08/2004

SCHEME 1: Synthesis of Novel Pentacene Derivatives 3a and 3b

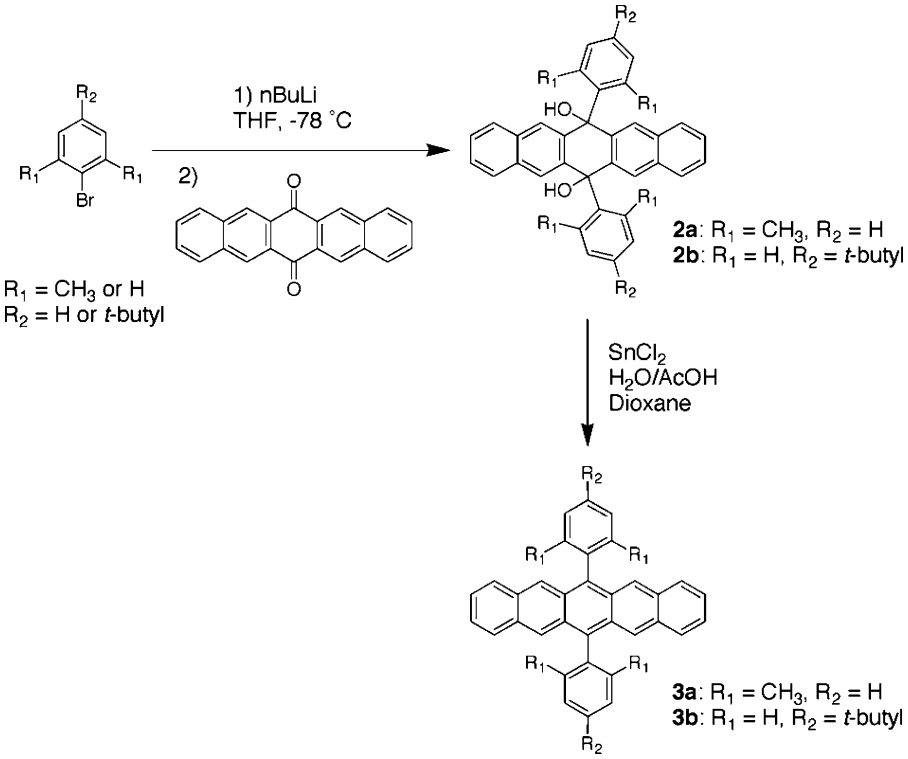

Experimental Section

General Procedures and Materials. All commercially available materials related to the synthesis of the pentacene derivatives were used without further purification, with the exception of THF, which was distilled over sodium and benzophenone. NMR spectra were recorded on a Brüker 300 MHz NMR spectrometer. ^{1}H and ^{13}C NMR samples were internally referenced to TMS (0.00 ppm). Flash chromatography was performed with 32−63 mesh silica gel. Quantitative Technologies Inc. (QTI) performed all elemental analyses. All organic materials used in the preparation of thin films or OLEDs were purified via two sequential train sublimation steps (∼4.0 × 10^{-6} Torr).

6,13-Diphenylpentacene **(1**, DPP) was synthesized as previously reported[27,28] and 6,13-bis(2,6-dimethylphenyl)pentacene (**3a**), and 6,13-bis(4-*tert*-butylphenyl)pentacene (**3b**) were prepared in a similar manner (Scheme 1). Substituted aryllithium reagents were generated by lithium−halogen exchange of the appropriate aryl bromide via treatment with *(n*-butyl)lithium. Introduction of the substituted phenyl groups proceeded in moderate yield (41−77%) upon addition of the freshly prepared (aryl)lithium reagents to 6,13-pentacenequinone. Diols **2a** and **2b** were then reduced to the desired pentacene by treatment with tin(II) chloride dihydrate in aqueous acetic acid. Purification of the pentacene derivatives was accomplished by chromatographic separation followed by duplicate train sublimation. Care was taken to ensure that the target compounds were not exposed to ambient light during the purification processes.

Preparation of Pentacenediols (2a Given as a Representative). A solution of 2-bromo-*m*-xylene (2.4 g, 13 mmol) in THF (35 mL) was stirred under N_2 and cooled to −78 °C in a dry ice/acetone bath. Upon cooling, (*n*-butyl)lithium (8.9 mL, 14.3 mmol) was added and the solution was stirred for 45 min to affect metal−halogen exchange. The yellow solution was then transferred via cannula to a flask containing a cooled (−78 °C) suspension of 6,13-pentacenequinone (0.4 g, 1.3 mmol) in THF (150 mL). The resulting solution was removed from the cold bath and allowed to attain room temperature. After 5 h at room temperature, the reaction mixture was transferred to a separatory funnel and quenched with 5% acetic acid (10 mL). The aqueous layer was extracted with ethyl acetate (20 mL), and the combined organic layers were dried with $MgSO_4$. The solvent was removed in vacuo until only ∼10 mL remained, at which point hexane (100 mL) was added, resulting in the formation of a white precipitate. The diol was isolated via vacuum filtration (0.52 g, 77% yield).

6,13-Bis(2,6-dimethylphenyl)-6,13-dihydropentacene-6,13-diol (2a): 77% yield; ^{1}H NMR ($CDCl_3$) δ 7.73 (s, 4H), 7.72−7.69 (dd, J = 6.2, 3.3 Hz, 4H), 7.44−7.38 (dd, J = 6.2, 3.3 Hz, 4H), 7.21 (m, 2H), 7.16−7.06 (m, 4H), 2.20 (s, 2H), 2.17 (s, 12H); ^{13}C NMR ($CDCl_3$) δ 143.7, 139.3, 137.9, 133.7, 131.3, 128.1, 127.5, 127.1, 126.5, 77.4, 15.5. Anal. Calcd for $C_{38}H_{32}O_2$: C, 87.66; H, 6.19. Found: C, 87.31; H, 6.08.

6,13-Bis(4-*tert*-butylphenyl)-6,13-dihydropentacene-6,13-diol (2b): 41% yield;^{1}H NMR ($CDCl_3$) δ 8.45 (s, 4H), 7.94−7.90 (dd, J = 6.1, 3.3 Hz, 4H), 7.56−7.53 (dd, J = 6.1, 3.3 Hz, 4H), 6.78 (d, J = 8.6 Hz, 4H), 6.72 (d, J = 8.6 Hz, 4H), 2.76 (s, 2H), 1.10 (s, 18H);^{13}C NMR ($CDCl_3$) δ 148.6, 140.2, 138.3, 132.6, 128.2, 127.2, 126.2, 125.1, 124.0, 75.7, 34.0, 31.1. Anal. Calcd for $C_{42}H_{40}O_2$: C, 87.46; H, 6.99. Found: C, 87.11; H, 7.00.

Preparation of Substituted Pentacenes (3a Given as a Representative). To a stirred solution of pentacenediol **2a** (0.52 g, 1.0 mmol) in 1,4-dioxane (75 mL) was added a suspension of tin(II) chloride dihydrate (8 g, 35.4 mmol) in a 1:1 H_2O:acetic acid mixture (15 mL total). The reaction mixture was wrapped in foil and heated to 50 °C for 5 h. The solvent was removed in vacuo, and the resulting purple-brown residue was dissolved in a 1:1 H_2O:$CHCl_3$ partition. Care was taken to ensure that the solution was exposed to minimal amounts of ambient light; extractions and chromatographic separations were carried out in vessels wrapped in foil. The organic layer was separated

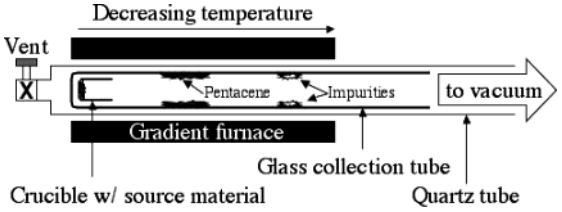

Figure 1. Schematic of vacuum train sublimation apparatus.

and washed with H_2O (3 × 150 mL), dried with $MgSO_4$, and concentrated in vacuo. Purification via flash chromatography (silica gel:$CHCl_3$) afforded 0.46 g of a fine deep purple powder (95.5% yield). The crude material was subjected to duplicate train sublimation (~3.0 × 10^{-6} Torr, 270−320 °C), yielding 0.27 g of pure product.

6,13-Bis(2,6-dimethylphenyl)pentacene (3a): 56% yield; ^{1}H NMR ($CDCl_3$) δ 8.13 (s, 4H), 7.76−7.72 (dd, J = 6.6, 3.4 Hz, 4H), 7.54−7.48 (m, 2H), 7.43−7.38 (m, 4H), 7.25−7.21 (dd, J = 6.6, 3.4 Hz, 4H), 1.81 (s, 12H); ^{13}C NMR ($CDCl_3$) δ 138.6, 138.4, 135.7, 131.7, 128.8, 128.2, 128.1, 127.9, 125.3, 124.9, 20.3. Anal. Calcd for $C_{38}H_{30}$: C, 93.79; H, 6.21. Found: C, 93.50; H, 6.06.

6,13-Bis(4-*tert*-butylphenyl)pentacene (3b): 31% yield;^{1}H NMR ($CDCl_3$) δ 8.36 (s, 4H), 7.76 (dd, J = 6.8, 3.1 Hz, 4H), 7.72 (d, J = 8.1 Hz, 4H), 7.56 (d, J = 8.1 Hz, 4H), 7.21 (dd, J = 6.8, 3.1 Hz, 4H), 1.56 (s, 18H); ^{13}C NMR ($CDCl_3$) δ 150.4, 136.9, 136.4, 131.4, 130.9, 128.8, 128.6, 125.6, 125.5, 124.9, 34.9, 31.6. Anal. Calcd for $C_{42}H_{38}$: C, 92.94; H, 7.06. Found: C, 92.81; H, 7.04.

Vacuum Train Sublimation. Following chromatographic purification, pentacenes **3a** and **3b** were thoroughly dried in a vacuum oven and then placed in a glass crucible fitted with a loose plug of glass wool. Crucibles containing between 0.1 and 0.5 g of crude material were then placed inside a cleaned glass tube (length ~60 cm, o.d. = 17 mm, i.d. = 15 mm) with one sealed end. The mouth of the crucible was pointed in the direction of the open end of the tube. The tube containing the crucible was then fitted into a larger quartz tube (length ~110 cm, o.d. = 25 mm, i.d. = 23 mm) connected to a mechanical pump and a diffusion vacuum pump on one end and a pressure release valve on the other. A 45 cm long section of copper tubing (o.d. = 31 mm, i.d. = 28 mm) fitted with a heater band was used as a gradient furnace that could be easily moved along the length of the quartz tube. The apparatus was slowly evacuated until a pressure of ~9.0 × 10^{-6} Torr was attained, at which point the furnace was placed over the crucible and heating was initiated (Figure 1). An Omega CN77330 Autotune PID Temperature Controller was used to regulate the temperature of the furnace, which was set at approximately 300 °C. Upon completion of sublimation, the apparatus was cooled to room temperature, vented, and disassembled. The glass tube was then cut at the appropriate place, and the purified microcystalline pentacene was removed from the interior of the tube. In most cases, samples were completely sublimed within 24 h and recovery rates ranged from 50 to 75%. All target molecules investigated within this study were doubly sublimed before use in composite films or OLEDs.

Spectroscopy of Solutions. UV−visible spectra were obtained on a Hewlett-Packard 8453 spectrophotometer (in the range 200−800 nm) using 1 cm quartz cells. Fluorescence was recorded from 500 to 800 nm on an ISA Fluorolog-3 (JY Horiba) with excitation and emission slit widths set at 1.0 nm. Dilute solutions (~1.0 × 10^{-6} M) of pentacenes **1**, **3a**, and **3b** were prepared using degassed spectroscopic grade solvents (toluene or chloroform) in evacuated and sealed cells. The relative fluorescence quantum yields, ϕ_{FL}, of these solutions were measured using Rhodamine 6G in ethanol (1.0 × 10^{-6} M, λ_{ex} = 488 nm, ϕ_r = 0.94) as a reference[30,31] and calculated using

$$\phi_s = \phi_r \frac{A_r(\lambda_r) I_r(\lambda_r) n_s^2}{A_s(\lambda_s) I_s(\lambda_s) n_r^2} \frac{D_s}{D_r} \quad (1)$$

Subscripts s and r denote sample and reference values respectively, $A(\lambda)$ denotes absorbance at the excitation wavelength, $I(\lambda)$ denotes lamp intensity at the prescribed wavelength, n denotes refractive index, and D denotes the integral of the emission spectrum. The refractive index was assumed to be equivalent to that of the pure solvent: 1.45 for chloroform and 1.36 for ethanol at room temperature.

Photooxidative Stability in Solution. Separate solutions of pentacenes **1** and **3a** (optical density of 1.2 and 0.1) were prepared in air-saturated toluene and placed in spectrophotometric cells. The cells were shielded from light until the experiment began, at which point an initial UV−vis spectrum was obtained. The cells were then placed on a benchtop exposed to air and ambient light. The solutions were scanned for their UV−vis spectrum at prescribed intervals until no absorbance in the visible region was evident.

Organic Light-Emitting Diode and Composite Thin Film Fabrication. Pre-cleaned glass substrates from Colorado Concept Coatings patterned with stripes of indium tin oxide (ITO) (100 nm thick with sheet resistance of 30 Ω/□) were used in the fabrication of organic light-emitting diodes (OLEDs). The substrates were washed with mild detergent then consecutively sonicated in detergent, deionized H_2O, acetone, and 2-propanol. Substrates were then vapor degreased over boiling 2-propanol, treated with oxygen plasma, and placed inside a vacuum deposition chamber. Devices were prepared by sequential vacuum vapor deposition[32] of the organic layers followed by vapor deposition of the Mg:Ag (~13:1) alloy cathode. The device structure for all OLEDs fabricated for this study is shown in Figure 2. The ITO served as the transparent anode and TPD (*N*,*N*′-diphenyl-*N*,*N*′-bis(3-methylphenyl)-1,1′-biphenyl-4,4′-diamine) was chosen for the hole-transporting layer (Figure 2). Alq_3 was used as both an electron-transporting layer and a host for the dispersed pentacene derivatives in the emitting layer. Materials were deposited in a vacuum chamber with a base pressure of 10^{-7} Torr in the following sequence: TPD (50 nm)/pentacene:Alq_3 (35 nm)/Alq_3 (35 nm)/Mg:Ag (120 nm). The active emitting layer was prepared by co-deposition of the guest and host materials evaporated from resistive heating furnaces. The rate of deposition of each material was monitored using a quartz crystal microbalance (nanogram sensitivity) to accurately determine the composition and thickness of the different layers. A shadow mask forming perpendicular stripes to the ITO was employed in the deposition of the cathode layer, resulting in four 2 × 2 mm^2 devices per substrate. Composite thin films containing solely the molecularly doped active emitting layer on fused silica (for spectroscopic characterization) were prepared in an identical manner as stated above. A calibrated quartz crystal monitor was used to determine the thickness of composite films (~750 nm).

Absolute Photoluminescence of Composite Thin Films. An integrating sphere (Labsphere Inc.) was used for the measurement of the absolute photoluminescence quantum yield, ϕ_{PL}, of molecularly doped thin films. Samples were subjected to UV excitation (λ = 325 nm) from a HeCd laser light source

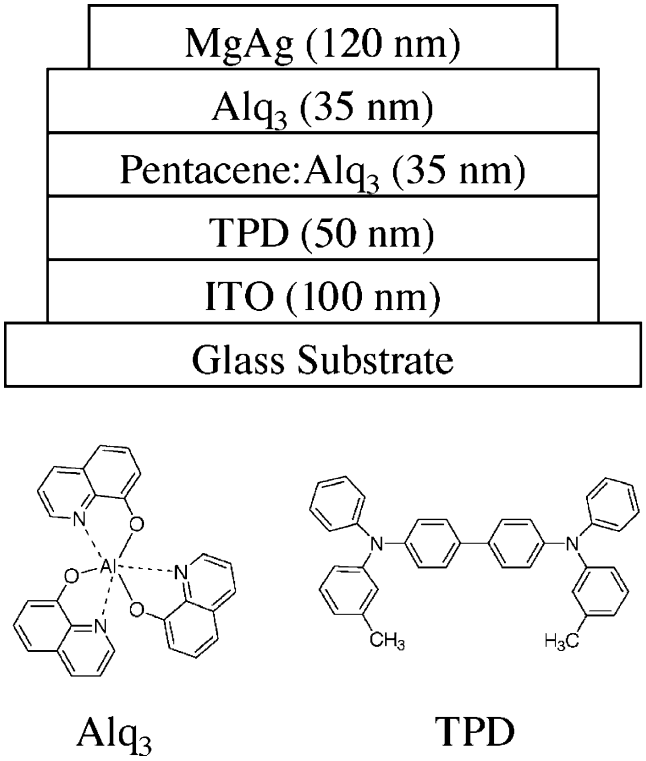

Figure 2. Device structure used in this study. TPD is used for the hole transporting layer whereas Alq_3 is used as both the electron-transporting layer and host in the emitting layer.

propagating through a fused silica fiber optic cable. A Kodak-Wratten 2B filter (wavelength cutoff at 385 nm) was used to filter out the excitation beam at the silicon photodiode detector. PL spectra were obtained both in situ, in vacuum, and ex situ, in a controlled atmosphere chamber filled with dry N_2 atmosphere using an ISA SpectrumOne CCD (JY Spex). Light intensity was measured with an IL1700 Research Radiometer (International Light). Quantum yields were calculated as previously reported after measuring the optical spectra of the films.[33]

Characterization of OLEDs. Current−voltage characteristics were measured on a Keithley 238 High Current Source Measure Unit. Electroluminescence (EL) spectra were obtained with an ISA SpectrumOne CCD (JY Spex). Current was measured as a function of voltage, which was adjusted from −7 to ∼20 V in 0.25 V increments. Light output was measured with a Minolta LS-110 Luminance Meter, and automated data acquisition was managed with Labview software. All measurements were carried out in an inert atmosphere (dry N_2).

Results and Discussion

Absorption and Emission in Solution. Figure 3 depicts the normalized absorption and fluorescence spectra of chloroform solutions of 2,6-dimethylphenyl-substituted pentacene (**3a**) and 6,13-bis(4-*tert*-butylphenyl)pentacene (**3b**). The absorption maxima of all three pentacenes (not shown for DPP) are nearly identical around 600 nm, but small differences are seen in the emission maxima ranging from 607 nm (**3a**) to 618 nm (**3b**). Very small Stokes shifts are evident for each pentacene derivative. The smallest Stokes shift measured only 6 nm for compound **3a**, suggesting that minimal molecular rearrangement takes place upon photoexcitation of the molecule. The emission of pentacene **3a** is slightly blue-shifted relative to that of the parent compound **1**, whereas compound **3b** exhibits a red shift in emission relative to that of **1**. As a result, pentacene **3b**

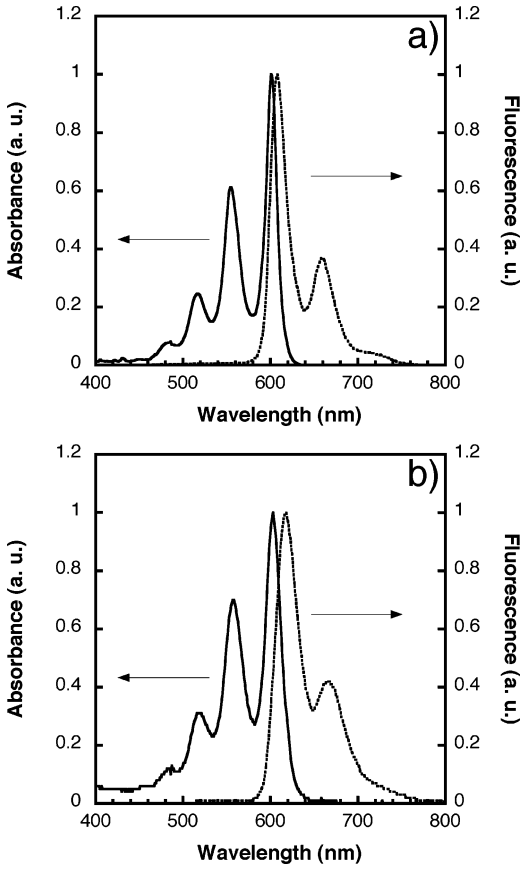

Figure 3. Normalized absorption (solid line) and fluorescence (dashed line) spectra of pentacenes **3a** (a) and **3b** (b) in chloroform.

TABLE 1: Absorption and Fluorescence Data for Pentacenes 1, 3a, and 3b

	in chloroform			in toluene		
compd	λ_{max}(abs), nm	λ_{max}(em), nm	ϕ_{FL}	λ_{max}(abs), nm	λ_{max}(em), nm	ϕ_{FL}
1	600	611	0.062	599	609	0.065
3a	601	607	0.063	601	604	0.076
3b	603	618	0.058	601	613	0.073

displays the largest Stokes shift. The optical characteristics of pentacenes **1**, **3a**, and **3b** measured in both chloroform and toluene are summarized in Table 1. All three compounds show similar fluorescence quantum yields ($\phi_{FL} < 0.10$) in solution when irradiated with 488 nm light. Comparable values were obtained upon irradiation with 505 or 530 nm light.

Photooxidative Stability in Solution. Polycyclic aromatic hydrocarbons such as pentacenes are notoriously unstable in solution when exposed to light and oxygen.[34,35] Previous studies on the diphenyl-substituted compound **1** have noted that photooxidation is characterized by formation of an endo peroxide bridge across the central ring at the reactive 6- and 13-positions of the pentacene unit.[27] We have studied the solution phase photooxidative stability of pentacenes **1** and **3a** by monitoring the change in their UV−vis absorption with time upon exposure to ambient room light and air. Newly synthesized pentacene **3a** exhibits roughly an order of magnitude slower rate for the loss of absorbance ($\lambda_{max} = 601$ nm) in toluene solution relative to compound **1**. Figure 4 shows a comparison of the rate of photobleaching of $\sim 2.0 \times 10^{-4}$ M solutions (initial optical density = 1.2) of pentacenes **1** and **3a** as monitored by the depletion of absorbance at their absorption maxima (λ_{max}) at 599 and 601 nm, respectively.[36] The decrease of absorbance in the visible region of the spectra is accompanied by the

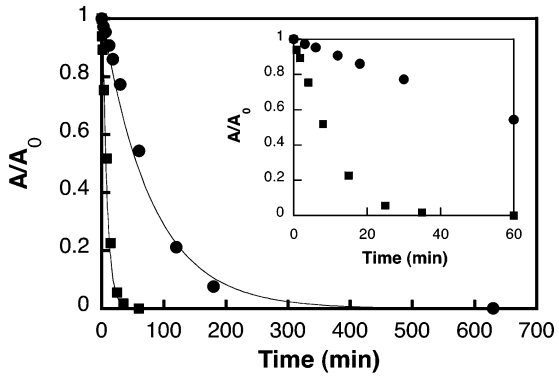

Figure 4. Loss of absorbance at λ_{max} versus time for pentacenes **1** (closed squares) and **3a** (closed circles) in toluene solution upon exposure to ambient light and air. The inset shows the photooxidation rate constants fit to an exponential decay: $k_1 = 2.32 \times 10^{-3}$ s^{-1}; $k_{3a} = 2.10 \times 10^{-4}$ s^{-1}.

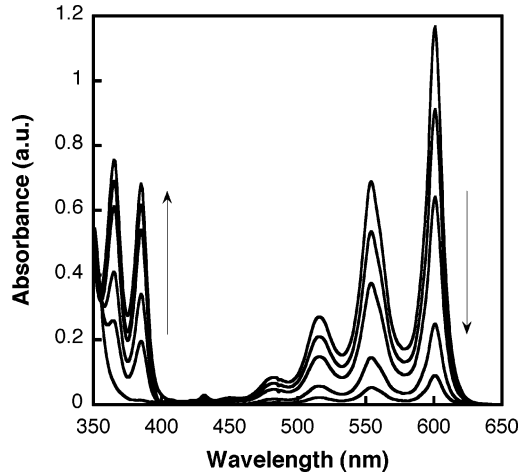

Figure 5. Change in UV−vis spectrum of pentacene **3a** upon exposure to light in ambient atmosphere after 0, 30, 60, 120, 180, and 630 min.

concomitant growth of two new peaks in the near UV (365 and 385 nm for pentacene **3a** in Figure 5) assigned to the photooxidation product. The loss of absorbance in the visible region due to the $\pi-\pi^*$ transition is consistent with the disruption of conjugation expected upon the formation of an endo peroxide across the central ring of the pentacene unit.[27] The photodegradation product(s) has(ve) neither been isolated nor characterized.

Examination of the molecular geometry of the pentacene molecules lends insight into the enhanced photooxidative stability of pentacene **3a** relative to pentacene **1**. It is well-known that the phenyl rings of substituted acene derivatives such as 9,10-diphenylanthracene are oriented perpendicular to the plane of the polyacene unit.[23,37] In the case of pentacene **3a**, the methyl groups are expected to lie above and below the reactive carbons at the 6- and 13- positions and as such may impede the approach of oxygen.

The solid-state photooxidative stability of neat pentacene films or pentacenes dispersed in the Alq_3 organic host was not investigated. It should be noted, however, that diaryl-substituted pentacenes are much more resistive to photooxidation in the solid state. Vacuum-sublimed residues of pentacenes **1**, **3a**, and **3b** showed no evidence of photooxidation even after prolonged exposure (>5 days) to ambient light and air.[38]

Absorption and Emission of Molecularly Doped Thin Films. Tris(quinolin-8-olato)aluminum(III) (Alq_3) was chosen as the host material for the pentacene derivatives because its

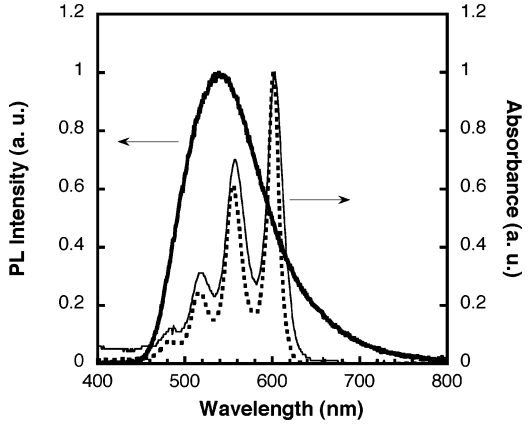

Figure 6. Photoluminescence spectrum of Alq_3 (bold line) and absorbance spectra of pentacenes **3a** (dashed line) and **3b** (normal line) showing good spectral overlap.

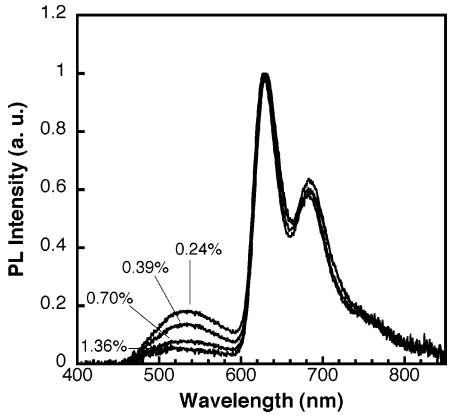

Figure 7. Normalized PL spectra of thin films of **3b** dispersed in Alq_3 at various dopant concentrations, expressed in mol %.

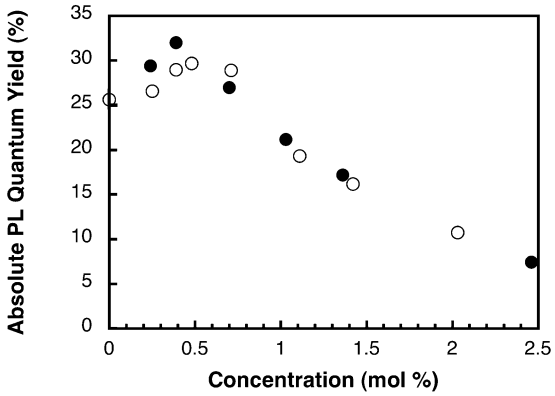

Figure 8. Absolute photoluminescence quantum yields of pentacenes **3a** (open circles) and **3b** (closed circles) dispersed in Alq_3 as a function of dopant concentration (in mol %).

green fluorescence spectrum overlaps well with the absorbance spectra of **3a** and **3b** (Figure 6). Strong spectral overlap is necessary for efficient Förster or Dexter energy transfer from host to guest molecules,[33] to ensure that light emission originates primarily from the guest pentacene molecules.

Figure 7 shows the PL spectra of films of *tert*-butylphenyl-substituted pentacene **3b** dispersed in Alq_3 at various dopant concentrations. The PL spectra are dominated by the red emission from the guest molecules (**3b**), reflecting good energy transfer from the host to the guest molecules.[33] The strongest emission is centered at 629 nm, which is red-shifted relative to the emission of pentacenes **1** (625 nm) and **3a** (618 nm). There is a small contribution (centered at 540 nm) from the Alq_3 host

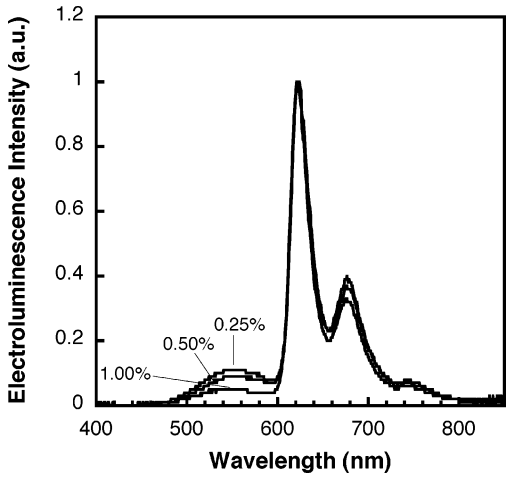

Figure 9. Change in EL spectra versus concentration for OLEDs containing pentacene **3a** in the active emitting layer.

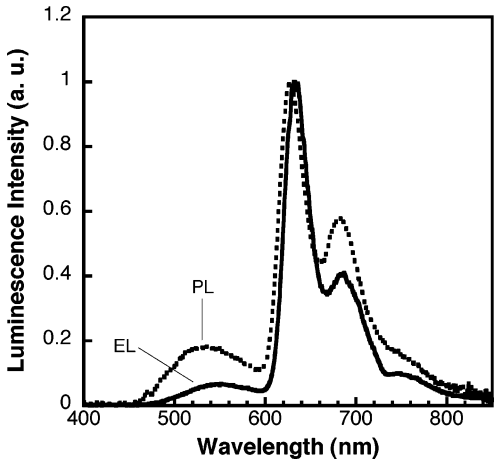

Figure 10. Electroluminescence (solid line) and photoluminescence (dashed line) spectra of active emissive layers containing 0.25 mol% pentacene **3b** in Alq_3.

that decreases as the concentration of the pentacene derivative increases. However, emission from the host is evident even at high molar concentrations (>2.0 mol %). Similar trends were observed for pentacene **3a** although the contribution of the Alq_3 emission was slightly larger at comparable guest molecule concentrations.

The absolute photoluminescence quantum yields measured for thin (~750 nm) films of pentacenes **3a** and **3b** dispersed in Alq_3 as a function of guest molecule concentration are shown in Figure 8. The maximum absolute photoluminescence quantum yields ($\phi_{PL} \sim 0.30-0.32$) were measured between 0.40 and 0.55 mol % for pentacene derivatives **3a** and **3b**, respectively. A similar PL quantum yield ($\phi_{PL} \sim 0.30$) was obtained for pentacene **1** at comparable guest molecule concentrations (0.55 mol %).[29] The decrease in ϕ_{PL} as the guest molar concentration increases is the result of aggregation and self-quenching.

Organic Light-Emitting Diodes. *(A) Electroluminescence Spectra.* The electroluminescence (EL) spectra of OLEDs based on an active emitting layer of pentacene **3a** doped in Alq_3 is depicted in Figure 9 for various guest molecule concentrations. The strongest emission peak is centered at 620 nm with a smaller peak at 676 nm and a shoulder at a longer wavelength. Devices based on pentacenes **1** and **3b** are red-shifted relative to **3a** and feature primary emission centered at 625 and 636 nm, respectively. The EL spectra are all similar to their PL counterparts, indicating emission from the same electronic excited state. Appreciable contribution from Alq_3 is observed at low dopant concentrations and is subsequently suppressed as the concentration of pentacene increases. Upon closer inspection, the contribution of the host in the PL spectra appears larger than in the EL spectra for a given guest molecule concentration.

Figure 10 compares the PL spectrum of a film of pentacene **3b** dispersed in Alq_3 and the EL spectrum of an OLED containing the same active emitting layer, showing a smaller contribution from the host emission in the EL spectrum. Similar observations were made between the PL and EL spectra of pentacenes **1**[26] and **3a**. The smaller contribution from the host in the EL spectra suggests that an additional mechanism besides energy transfer from host to guest molecules, which is the only operative PL mechanism, is taking place. Pentacene molecules may be acting as a charge trap and a direct recombination site for holes and electrons.[26] This additional EL mechanism has been previously demonstrated in other guest:host systems and has led to very efficient and stable OLEDs.[39,40]

The color purity of the pentacene-based OLEDs is dictated by the full width at half-maximum (fwhm) of the emission of the dopant molecule. The concentration of the pentacene derivative in Alq_3 also affects the color purity due to the presence of Alq_3 host emission in the EL spectrum. Figure 11 and Table 2 show the CIE (Commission Internationale de l'Eclairage) coordinates for the OLEDs characterized in this study. The current standard for red-emitting phosphors with regard to HDTV is $x = 0.64$ and $y = 0.33$. Pentacene **1** displays saturated red emission at a low molar concentration of 0.55% whereas pentacene **3a** has similar CIE coordinates, but at higher concentrations (1.5 mol %, $x = 0.64$, $y = 0.34$). Bis(4-*tert*-butylphenyl)pentacene **3b** shows a purer red color as its molar concentration increases, reaching $x = 0.68$ and $y = 0.31$ at 1.46 mol %.

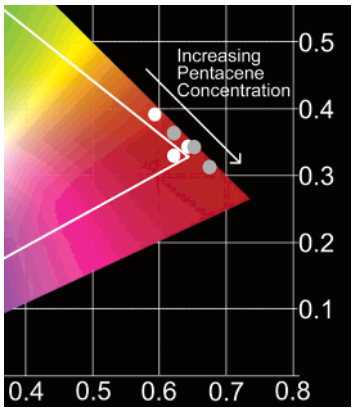

Figure 11. Change in CIE coordinates with increasing guest molecule concentration for OLEDs containing pentacene **3a** (white circles) and **3b** (gray circles).

TABLE 2: CIE Coordinates for OLEDs Containing Varying Concentrations of Pentacenes 1, 3a, and 3b in the Active Emitting Layer

pentacene	concn, mol %	*X*	*Y*
1	0.25	0.57	0.40
1	0.55	0.64	0.34
1	1.20	0.64	0.34
3a	0.26	0.59	0.39
3a	0.49	0.62	0.33
3a	1.38	0.64	0.34
3b	0.27	0.62	0.36
3b	0.47	0.65	0.34
3b	1.46	0.68	0.31

(B) Current Density−Voltage-Luminance Characterization. Representative current density−voltage luminance curves for

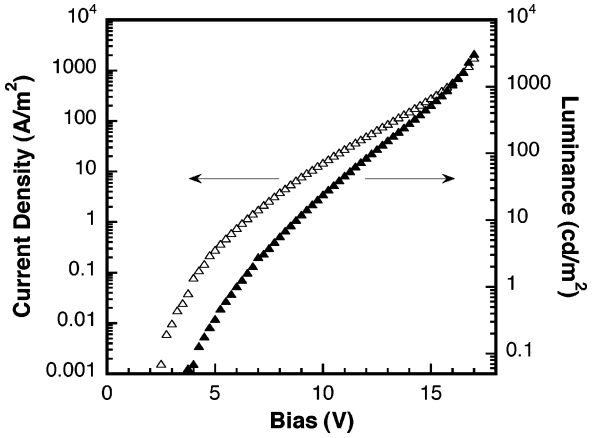

Figure 12. Luminance (L, filled triangles) and current density (J, open triangles) versus bias voltage for an OLED featuring an emitting layer of 0.47 mol % pentacene **3b**:Alq_3.

an OLED device with an emitting layer containing 0.47 mol % pentacene **3b** in Alq_3 are shown in Figure 12. The turn-on voltage (arbitrarily defined as the voltage required for a luminance of 0.1 cd/m^2)[12] for the device is <5 V. A luminance >3000 cd/m^2 was measured at 17 V and similar brightness was obtained for all the devices within the series at low dopant concentrations. Devices based on pentacene **3a** typically yielded the highest values for maximum brightness. The brightness attained at a given voltage decreases as a function of the guest molecule concentration, in part due to a decrease in the Alq_3 host emission as well as concentration quenching of interacting guest molecules. Because the maximum brightness (cd/m^2) is adjusted by multiplying the EL spectrum of an OLED device by the eye's photopic response, green emission from Alq_3 yields a significant contribution to the total luminance even when only a small peak is present in the spectrum. Therefore, at low guest molecule concentrations, greater luminance values can be expected because of the relatively large contribution from the Alq_3 host material. As the guest molecule concentration increases, there is a corresponding decrease in the green emission component.

In addition, an increase in the pentacene concentration produces a corresponding increase in the turn-on and operating voltages; this is consistent with the guest molecule acting as a charge carrier trap. For instance, devices based on pentacene **3b** show an escalation in turn-on voltage from 3.5 V at 0.25 mol % to 6.0 V at 2.52 mol %. Similar turn-on voltages were observed for OLEDs based on each of the different pentacenes employed in this study, suggesting that the EL mechanism is very similar for all three pentacenes. Increasing molar concentration also results in higher driving voltages required to attain specific current densities (Figure 13). For OLEDs based on pentacene **3a**, a current density of 100 A/m^2 is reached at 12.25 and 19.75 V for devices based on a low (0.26 mol %) and high (1.87 mol %) guest molecule concentration, respectively.

(C) EL Quantum Efficiency. The external electroluminescence quantum efficiencies (η_{EL}) at 100 A/m^2 of devices based on pentacenes **3a** and **3b** as a function of guest molecule concentration are shown in Figure 14. A similar but not identical concentration dependence to that measured for the PL quantum yields of the corresponding molecularly doped thin films (Figure 8) is observed. OLEDs based on either compound display maximum external EL quantum efficiencies at low molar concentrations (<1 mol %) of pentacene derivatives in Alq_3. Devices featuring an emitting layer comprising 0.47 mol % pentacene **3b** in Alq_3 displayed an external EL quantum

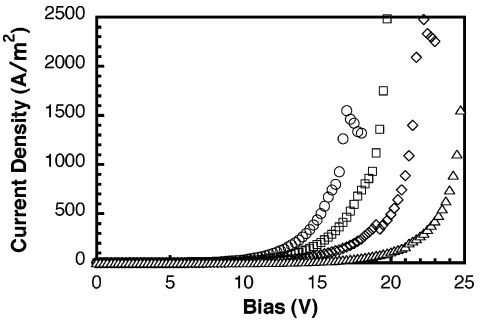

Figure 13. Current density versus bias voltage for OLEDs containing increasing molar concentrations of pentacene **3a** in Alq_3: 0.26 mol % (circles), 0.65 mol % (squares), 0.88 mol % (diamonds), and 1.87 mol % (triangles).

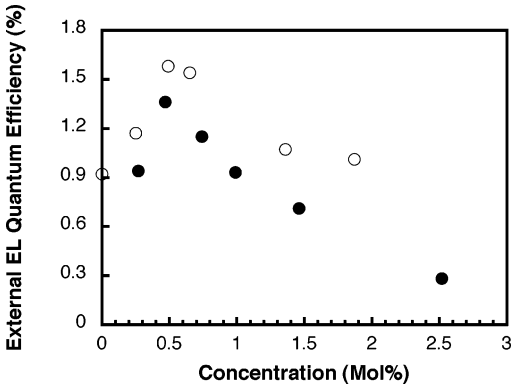

Figure 14. External EL quantum efficiency vs molar concentration of pentacene derivatives [**3a** (open circles), **3b** (closed circles)] in Alq_3 at a current density of 100 A/m^2.

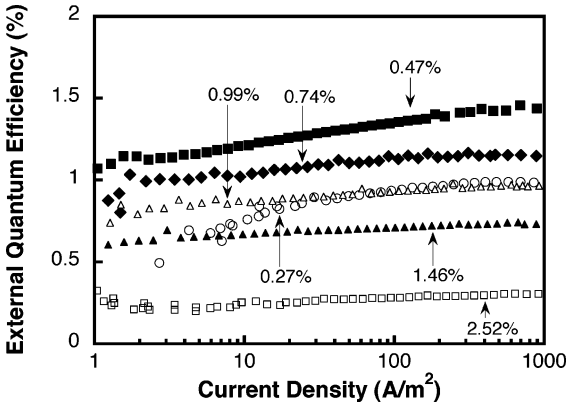

Figure 15. External EL quantum efficiency vs current density for OLEDs featuring pentacene **3b**; 0.27 mol % (open circles), 0.47 mol % (filled squares), 0.74 mol % (filled diamonds), 0.99 mol % (open triangles), 1.46 mol % (filled triangles), 2.52 mol % (open squares) dispersed in Alq_3 as the active emissive layer.

efficiency of ~1.4%. The optimal molar concentration for OLEDs based on pentacene **1** was found at 0.25 mol %; the device yielded η_{EL} ~1.4%.[26] The most efficient devices were the ones containing pentacene **3a**, which showed a maximum η_{EL} ~1.6% at a dopant concentration of 0.49 mol %. A decrease in the η_{EL} is observed as the pentacene concentration in the emitting layers increases.

The maximum η_{EL} determined for devices based on pentacenes **1**, **3a**, and **3b** seems to approach the theoretical limit.[41] The external EL quantum efficiency may be expressed by the equation $\eta_{EL} = \alpha\gamma\eta_r\phi_{PL}$, where α is the light output coupling factor ($\alpha = 1/2n^2$, n = refractive index), γ is the probability of carrier recombination, η_r is the production efficiency of excitons, and ϕ_{PL} is the absolute PL quantum yield of the emitter.

Assuming $\alpha = 0.20$ ($n = \sim 1.7$ for Alq_3),[42] $\gamma = 1.0$, and $\eta_r = 0.25$ for singlet excitons,[15,43] and on the basis of the measured $\phi_{PL} = 0.32$, the η_{EL} theoretical limit for an OLED device, based on 0.47 mol % pentacene **3b** in Alq_3, is 1.6%. The observed value of approximately 1.4% is slightly smaller than the theoretical limit (which is subject to the validity of the above-mentioned assumptions).[44] The observed external EL quantum efficiencies for devices based on the three pentacene derivatives were nearly constant over a wide range of current densities. Figure 15 illustrates that η_{EL} changes very little from current densities of $1-1000$ A/m^2 for OLEDs based on pentacene **3b** for dopant concentrations ≥ 0.50 mol %. This is an attractive and important feature for an OLED device especially for applications that require stable and high current densities for operation (i.e., passive matrix displays or solid-state lasers). In addition, the stability in the EL quantum efficiency and color over a wide range of current densities is important in any application that requires simultaneous control of RGB (red, green, and blue) color emission over a wide range of current densities.

Conclusions

We have synthesized and characterized two new pentacene derivatives based on pentacene **1** (DPP). Pentacene **3a** displayed enhanced photooxidative stability in toluene solutions relative to pentacene **1** due to the steric effects of the methyl groups. Red emission from pentacenes **1**, **3a**, and **3b** dominated the PL spectra of their composite thin films and was attributed to efficient Förster energy transfer from the Alq_3 host molecules to the pentacene guest molecules. The EL and PL spectra based on composite thin films containing pentacenes **3a** and **3b** were similar, suggesting emission from the same electronic excited states. A smaller contribution from the host was observed for a given dopant concentration in the EL versus PL spectra, revealing that an additional EL mechanism besides energy transfer is taking place, which was attributed to direct recombination of holes and electrons on the dopant molecules.

By controlling the dopant concentration of the emitting layer in pentacene-based OLEDs, fine-tuning of the red emission was achieved. The CIE color coordinates of OLEDs containing 0.47 mol % of pentacene **3b** (0.64, 0.34) or 1.50 mol % pentacene **3a** (0.64, 0.34) closely match the requirements set for red emission in high definition television (HDTV). The external EL quantum efficiencies of OLEDs based on pentacene derivatives are nearly constant across a wide range of current densities, which is important for display and solid-state lighting applications. The maximum η_{EL} for devices based on pentacenes **1**, **3a**, and **3b** approaches the theoretical limit on the basis of the measured PL quantum yields (0.30−0.32). We are currently developing new pentacene derivatives to optimize the PL quantum yield, and in turn improve the device EL quantum efficiency.

Acknowledgment. This work was supported by the Office of Naval Research. We thank Hedi Mattoussi and Charles Merritt for use of the spectrofluorimeter. M.W. acknowledges the National Research Council for administering the NRC post-doctoral fellowship program at the Naval Research Laboratory.

References and Notes

(1) Mitschke, U.; Bauerle, P. *J. Mater. Chem.* **2000**, *10*, 1471.
(2) Shirota, Y. *J. Mater. Chem.* **2000**, *10*, 1.
(3) Hosokawa, C.; Higashi, H.; Nakamura, H.; Kusumoto, T. *Appl. Phys. Lett.* **1995**, *67*, 3853.
(4) Tang, C. W.; VanSlyke, S. A.; Chen, C. H. *J. Appl. Phys.* **1989**, *65*, 3610.
(5) Hamada, Y.; Kanno, H.; Tsujioka, T.; Takahashi, H. *Appl. Phys. Lett.* **1999**, *75*, 1682.
(6) Jung, B.; Yoon, C.; Shim, H.; Do, L.; Zyung, T. *Adv. Funct. Mater.* **2001**, *11*, 430.
(7) Xie, Z. Y.; S., H. L.; Lee, S. T. *Appl. Phys. Lett.* **2001**, *79*, 1048.
(8) O'Brien, D. F.; Baldo, M. A.; Thompson, M. E.; Forrest, S. R. *Appl. Phys. Lett.* **1999**, *74*, 442.
(9) Gao, F. G.; Bard, A. J. *J. Am. Chem. Soc.* **2000**, *122*, 7426.
(10) Lamansky, S.; Djurovich, P.; Murphy, D.; Abdel-Razzaq, F.; Lee, H.; Adachi, C.; Burrows, P. E.; Forrest, S. R.; Thompson, M. E. *J. Am. Chem. Soc.* **2001**, *123*, 4304.
(11) Kawamura, Y.; Yanagida, S.; Forrest, S. R. *J. Appl. Phys.* **2002**, *92*, 87.
(12) Gong, X.; Ostrowski, J. C.; Bazan, G. C.; Moses, D.; Heeger, A. J.; Liu, M. S.; Jen, A. K.-Y. *Adv. Mater.* **2003**, *15*, 45.
(13) Duan, J. P.; Sun, P. P.; Cheng, C. H. *Adv. Mater.* **2003**, *15*, 224.
(14) Baldo, M. A.; O'Brien, D. F.; You, Y.; Shoustikov, A.; Sibley, S.; Thompson, M. E.; Forrest, S. R. *Nature* **1998**, *395*, 151.
(15) Baldo, M. A.; O'Brien, D. F.; Thompson, M. E.; Forrest, S. R. *Phys. Rev. B* **1999**, *60*, 14422.
(16) Baldo, M. A.; Adachi, C.; Forrest, S. R. *Phys. Rev. B* **2000**, *62*, 10967.
(17) Szmytkowski, J.; Stampor, W.; Kalinowski, J.; Kafafi, Z. H. *Appl. Phys. Lett.* **2002**, *80*, 1465.
(18) Young, R. H.; Tang, C. W.; Marchetti, A. P. *Appl. Phys. Lett.* **2002**, *80*, 874.
(19) Anthony, J. E.; Brooks, J. S.; Eaton, D. L.; Parkin, S. R. *J. Am. Chem. Soc.* **2001**, *123*, 9482.
(20) Anthony, J. E.; Eaton, D. L.; Parkin, S. R. *Org. Lett.* **2001**.
(21) Afzali, A.; Dimitrakopoulos, C. D.; Breen, T. L. *J. Am. Chem. Soc.* **2002**, *124*, 8812.
(22) Miller, G. P.; Mack, J. *Org. Lett.* **2000**, *2*, 3979.
(23) Miller, G. P.; Mack, J.; Briggs, J. *Org. Lett.* **2000**, *2*, 3983.
(24) Dimitrakopoulos, C. D.; Malenfant, P. R. L. *Adv. Mater.* **2002**, *14*, 99.
(25) Tokumoto, T.; Brooks, J. S.; Clinite, R.; Wei, X.; Anthony, J. E.; Eaton, D. L.; Parkin, S. R. *J. Appl. Phys.* **2002**, *92*, 5208.
(26) Picciolo, L. C.; Murata, H.; Kafafi, Z. H. *Appl. Phys. Lett.* **2001**, *78*, 2378.
(27) Allen, C. F. H.; Bell, A. *J. Am. Chem. Soc.* **1942**, *64*, 1253.
(28) Maulding, D. R.; Roberts, B. G. *J. Org. Chem.* **1969**, *34*, 1734.
(29) Picciolo, L. C.; Murata, H.; Kafafi, Z. Derivatives of polyaromatic hydrocarbons as red emitters in organic light emitting devices. *Proc. SPIE-Int. Soc. Opt. Eng.* **2001**.
(30) Fischer, M.; Georges, J. *Chem. Phys. Lett.* **1996**, *260*, 115.
(31) Lakowicz, J. R. *Principles of Fluorescence Spectroscopy*, 2nd ed.; Plenum Publishers: New York, 1999.
(32) Forrest, S. R. *Chem. Rev.* **1997**, *97*, 1793.
(33) Mattoussi, H.; Murata, H.; Merritt, C. D.; Iizumi, Y.; Kido, J.; Kafafi, Z. H. *J. Appl. Phys.* **1999**, *86*, 2642.
(34) Malkin, J. *Photophysical and Photochemical Properties of Aromatic Compounds*; CRC Press: Boca Raton, FL, 1992.
(35) Sakai, K.-I.; Ohshima, S.; Uchida, A.; Oonishi, I.; Fujisawa, S.; Nagashima, U. *J. Phys. Chem.* **1995**, *99*, 5909.
(36) Photooxidation of dilute solutions ($\sim 1.7 \times 10^{-5}$ M) yielded approximately the same relative difference in the rate constants for the two compounds.
(37) Becker, H.-D.; Langer, V.; Sieler, J.; Becker, H.-C. *J. Org. Chem.* **1992**, *57*, 1883.
(38) Solid films of pentacenes were exposed to ambient light and air for 5 or more days, at which point the material was dissolved in chloroform and UV−vis spectra were obtained. For each pentacene, the newly obtained spectra were identical to the initial spectra for pure pentacenes; there were no peaks in the near UV that could be assigned to photooxidation products.
(39) Murata, H.; Merritt, C. D.; Kafafi, Z. H. *IEEE J. Sel. Top. Quantum Electron* **1998**, *4*, 119.
(40) Shaheen, S. E.; Kippelen, B.; Peyghambarian, N.; Wang, J.-F.; Anderson, J. D.; Mash, E. A.; Lee, P. A.; Armstrong, N. R.; Kawabe, Y. *J. Appl. Phys.* **1999**, *85*, 7939.
(41) Tsutsui, T. *MRS Bull.* **1997**, *22*, 39.
(42) Greenham, N. C.; Friend, R. H.; Bradley, D. D. C. *Adv. Mater.* **1994**, *6*, 491.
(43) Brown, A. R.; Pichler, K.; Greenham, N. C.; Bradley, D. D. C.; Friend, R. H.; Holmes, A. B. *Chem. Phys. Lett.* **1993**, *210*, 61.
(44) Kalinowski, J.; Palilis, L. C.; Kim, W. H.; Kafafi, Z. H. *J. Appl. Phys.* **2003**, *94*, 7764.